

## Katdetectr: An R/Bioconductor package utilizing unsupervised changepoint analysis for robust kataegis detection

--Manuscript Draft--

<b>Manuscript Number:</b>	GIGA-D-23-00051R1	
<b>Full Title:</b>	Katdetectr: An R/Bioconductor package utilizing unsupervised changepoint analysis for robust kataegis detection	
<b>Article Type:</b>	Technical Note	
<b>Funding Information:</b>	Daniel den Hoed Fonds (DDHF-CCBC)	Dr Harmen van de Werken
<b>Abstract:</b>	<p><b>Background</b>            Kataegis refers to the occurrence of regional genomic hypermutation in cancer and is a phenomenon that has been observed in a wide range of malignancies. A kataegis locus constitutes a genomic region with a high mutation rate, i.e., a higher frequency of closely interspersed somatic variants than the overall mutational background. It has been shown that kataegis is of biological significance and possibly clinically relevant. Therefore, an accurate and robust workflow for kataegis detection is paramount.</p> <p><b>Findings</b>            Here we present Katdetectr, an open-source R/Bioconductor-based package for the robust yet flexible and fast detection of kataegis loci in genomic data. In addition, Katdetectr houses functionalities to characterize and visualize kataegis and provides results in a standardized format useful for subsequent analysis. In brief, Katdetectr imports industry-standard formats (MAF, VCF, and VRanges), determines the intermutation distance of the genomic variants and performs unsupervised changepoint analysis utilizing the Pruned Exact Linear Time search algorithm followed by kataegis calling according to user-defined parameters. We used synthetic data and an a priori labeled pan-cancer dataset of whole genome sequenced malignancies for the performance evaluation of Katdetectr and five publicly available kataegis detection packages. Our performance evaluation shows that Katdetectr is robust regarding tumor mutational burden (TMB) and shows the fastest mean computation time. Additionally, Katdetectr reveals the highest accuracy (0.99, 0.99) and normalized Matthews Correlation Coefficient (0.98, 0.92) of all evaluated tools for both datasets.</p> <p><b>Conclusions</b>            Katdetectr is a robust workflow for the detection, characterization, and visualization of kataegis and is available on Bioconductor: <a href="https://doi.org/doi:10.18129/B9.bioc.katdetectr">https://doi.org/doi:10.18129/B9.bioc.katdetectr</a></p>	
<b>Corresponding Author:</b>	Harmen van de Werken Erasmus MC Rotterdam, Select State NETHERLANDS	
<b>Corresponding Author Secondary Information:</b>		
<b>Corresponding Author's Institution:</b>	Erasmus MC	
<b>Corresponding Author's Secondary Institution:</b>		
<b>First Author:</b>	Daan Hazelaar	
<b>First Author Secondary Information:</b>		
<b>Order of Authors:</b>	Daan Hazelaar	
	Job van Riet	
	Youri Hoogstrate	
	Harmen van de Werken	
<b>Order of Authors Secondary Information:</b>		

**Response to Reviewers:**

Please note that we have added a supplementary pdf file that contains our response to the editor and the reviewers. This supplementary files contains mathematical expressions which we use in our response to the reviewers.

Concerning: GIGA-D-23-00051 and detailed response to its review

Dear Hongling Zhou,

Thank you very much for the thorough evaluation of our manuscript GIGA-D-23-00051 entitled: "Katdetectr: An R/Bioconductor package utilizing unsupervised changepoint analysis for robust kataegis detection" by Daan Hazelaar; Job van Riet; Youri Hoogstrate; Harmen van de Werken.

We greatly appreciate the opportunity to revise our manuscript according to the high-quality reports of the reviewers. We include a point-by-point reply to the criticism and suggestions by the reviewers and you. Moreover, the described changes are indicated with track changes in the resubmitted manuscript.

1. Register any new software application in the bio.tools and SciCrunch.org databases to receive RRID (Research Resource Identification Initiative ID) and biotoolsID identifiers, and include these in your manuscript.

Dear dr. Hongling Zhou, we have registered katdetectr on bio.tools (biotoolsID: katdetectr) and SciCrunch.org (RRID: SCR\_023506) and added the accompanying identifiers to the manuscript under the section: Availability and requirements in compliance with the GIGA journal requirements.

2. Computational workflows should be registered in workflowhub.eu and the DOIs cited in the relevant places in the manuscript.

We have registered katdetectr (10.48546/workflowhub.workflow.463.1) and the performance evaluation of katdetectr (10.48546/workflowhub.workflow.500.1) on workflowhub.eu and added the corresponding to the availability and requirements section in the manuscript.

Sincerely yours,

Harmen J. G. van de Werken, Ph.D.  
Assistant Professor in Computational Biology & Bioinformatics in Immunology and Cancer at the Erasmus Medical Center in the Department of Immunology

Reviewer #1: minor revision

In this short manuscript, Hazelaar et al. describe a new software package written in R, called "katdetectr". This package can be useful as an addition to existing computational tools for identifying and characterizing kataegis in cancer genomes. The paper then compares katdetectr favorably against other software for detecting kataegis, using synthetic and real cancer data. Overall, the paper is fine and the katdetectr package is a nice addition for researchers' toolbox. I would suggest that the authors make the following improve-ments.

1. Choose a convention for decimal point and digit separator, then stick with it. "." was

used as both the decimal point and digit separator for large numbers, which gets confusing. Typically, "." is used for decimal point and "," is used for digit separator.

We thank the reviewer for this editorial comment. We have indeed revised our manuscript (and figures) in accordance the convention of using "." as a decimal point and using "," as a digit separator. We apologize for the previous oversight.

2. The Introduction is so abbreviated that it doesn't serve much purpose. Either flesh it out with more information or just drop it completely. This journal accepts papers that go right into re-sults, so it's fine. But the authors should also consider if writing a more expansive introduction can make the paper more accessible to readers who aren't already as knowledgeable.

According to the reviewer's suggestion, we have extended the introduction to improve this manu-script's accessibility for readers not yet familiar with kataegis. Additionally, we have included additional references within the introduction to promote further reading into the current state of re-search regarding kataegis (lines 60 - 78).

3. The biggest issue is using the 2013 Alexandrov kataegis calls as "ground truth" when multi-ple packages published since then detect 102 loci that Alexandrov (2013) missed. Seems like it would be much more sensible to use the calls from the 2020 PCAWG paper instead: <https://doi.org/10.1038/s41586-020-1969-6>. The data are controlled access, but it should be possible to get them.

Whilst we agree with the reviewer that utilizing the latest release of the kataegis calls (as called within the PCAWG) would be a worthwhile endeavor as the PCAWG-calls would indeed be more recent and potentially contain improved annotations. However, this dataset is currently (as mentioned) only available under controlled-access whilst the Alexandrov et al. call-set is publicly available.

In line with the philosophy of open science and Giga Science, we believe that reproducible and continued benchmarking of novel computational methodology against comparable methodology is paramount and that this is restricted when controlled-access data is involved.

Therefore, we used the publicly-available dataset as described by Alexandrov et al. (2013) for benchmarking which allowed us to co-publish our input data and results for public review and future comparison without restriction.

To overcome the potential inaccuracy of the employed ground-truth call-set, we compared the evaluated methodologies without the dependence of the "ground-truth" labels by employing a Venn diagram (Fig. 2b) which highlights the (shared) dis/concordance against the "ground-truth". This allows for a visual comparison of the packages which is less dependent on the input.

We have extended and refined our discussion to address these valid concerns on the employed "ground-truth" set (lines 287 - 289).

4. Katdetectr does outperform other packages for high TMB samples ( $\geq 10$ ). But those are rela-tively few ( $< 10\%$  of samples). Should state this clearly in text.

We have added the number of currently-investigated WGS samples with a  $TMB \geq 10$  ( $n = 20$ ) to our manuscript (line 186).

The large pan-cancer analysis by Priestley et al. (2019)[1] on metastatic cancers revealed that 17.7% of examined malignancies reveal  $TMB \geq 10$  and that this is not a rare occurrence for several malignancies. In particular, metastatic skin and lung

malignancies reveal 55-60% cases with such elevated TMB. We have further elaborated these potential use-cases within our discussion (line 260 - 261).

[1] Priestley P, Baber J, Lolkema MP, et al. Pan-cancer whole-genome analyses of metastatic solid tumours. *Nature*. 2019;575(7781):210-216. doi:10.1038/s41586-019-1689-y

5. The runtime data would be better represented by violin plots. Having many data points bunched together isn't helpful to visualize the distributions.

As per reviewer request, we have replaced the boxplots in fig. 2C and suppl. fig. 2 with violin plots and individual data-points.

6. I tested the katdetectr package and noticed something peculiar about the documentation. In section 6 "More parameter settings", there's a disclaimer that the developers did not test such settings. Doesn't seem like a good practice to put that in there if the devs themselves don't know how the function will behave.

We thank the reviewer for extensively investigating katdetectr and commenting on the accompanying vignette.

We would like to emphasize that we have thoroughly tested all available functions presented within katdetectr (incl. unit-testing) to ensure future sanity and proper function. In addition, katdetectr adheres to the BioConductor guidelines and follows their formal programmatic style, testing and documentation.

We merely wished to highlight additional functionality of the presented methodology and the flexibility of the user-available parameters by showcasing an additional use-case involving clustered mutations which do not necessarily adhere to the canonical kataegis ruleset. Whilst we ensured that these additional results were sane, we did not perform an extensive evaluation and comparison of these additional functionalities similar to those we performed for the detection of kataegis.

We agree with the reviewer that this could be misconstrued and derailing from the main functionality of katdetectr, as evaluated within this manuscript, and have removed this section from the vignette.

We updated katdetectr on BioConductor, but please note that the Bioconductor release branch is only updated twice per year (incl. the change in the vignette). The most current version of katdetectr which already includes this change is available from GitHub: <https://github.com/ErasmusMC-CCBC/katdetectr>

Reviewer #2: major revision

This manuscript presents a clever tool of hypermutation detection with changepoint analysis-based R languages, katdetectr. The authors have constructed the R package based on the changepoint package of Killick and Eckley.

1. In the mutation processing step, the author stated that "the imported variants are pre-processed such that, per chromosome, all variants are sorted in ascending order based on their genomic position. Overlapping variants are merged into a single record." What does "all variants" refer to?

With all variants, we referred to all the genomic variants as supplied by the user within their VCF, MAF or user-curated VRanges object. Users can perform pre-filtering of

genomic variants by utilizing the VRanges object (e.g., as generated from a VCF) and supplying this VRanges into the kataegis detection method. This VRanges can house SNVs, (long) InDels and structural variants and all will be used for downstream kataegis detection if present.

We apologize for the previous omission of details and have extended this within our manuscript (line 358 - 359).

2. Are other variants, e.g., long Indel and structure variation included?

As also mentioned in the previous comment (#1), all forms of genomic variants can be supplied to katdetectr and used for subsequent kataegis detection. The presented analysis and evaluation of kataegis calls as presented within this manuscript was performed on SNVs-only as at least one package only imported SNVs.

Katdetectr merges (partially) overlapping genomic variants (regions) using IRanges::reduce() and from this generates a single record with the 5'-most shared position as reference anchor (start position), an X as reference allele, XX as alternative allele and containing information detailing which variant records were merged.

However, it would be advisable to filter all or large (e.g., >1kb) structural variations beforehand as these could potentially overlap with many (smaller) genomic variants resulting in a potential loss of kataegis detection.

We have extended our methodology with these details on merging overlapping variants (line 358 - 360)

3. How do the other tools deal with such variants, and what's your consideration for this treatment?

To better address this interesting question, we performed an investigation on how the alternative packages handle (long) and overlapping variants as the respective papers, manuscripts, vignettes and manuals lack much (if any) detail on this topic.

We added an additional script to our public repository which we used to assess the behavior of these packages regarding overlapping variants:  
[https://github.com/ErasmusMC-CCBC/evaluation\\_katdetectr/blob/main/notebooks/R/checking\\_overlapping\\_variants.Rmd](https://github.com/ErasmusMC-CCBC/evaluation_katdetectr/blob/main/notebooks/R/checking_overlapping_variants.Rmd)

With this script, we generated a small synthetic sample-set of (non-)overlapping variants:

- 1 InDel (1200 kb)
- 10 random SNVs
- 10 kataegis SNVs
- 9 SNVs that overlap with one or more of the previous
- 10 SNVs at exactly the same genomic location

If no merging is performed, 40 variants should be present in the resulting data-tables. If merging is performed (such as in katdetectr), only 22 variants should be present. This allows us to empirically determine the (default) behavior of the packages as the documentation and respective application notes are scarce on details regarding overlapping variants.

Please see below, comment #4, for the details of this analysis. In summary, none of the (other) evaluated packages performed merging of overlapping variants.

Maftools

We did not find relevant parameters regarding overlapping variants and no reference to overlapping variants in the documentation, paper or manual of this tools.

From our test-set, we observed that the overlapping variants are not merged.

#### SeqKat

We did not find relevant parameters regarding overlapping variants and no reference to overlapping variants in the documentation, paper or manual of this tools. SeqKat furthermore only allows the import of a BED file containing SNVs, disregarding anything larger than 1bp.

From our remaining test-set of SNVs-only, we observed that the overlapping variants are not merged.

#### ClusteredMutations

We did not find relevant parameters regarding overlapping variants and no reference to overlapping variants in the documentation, paper or manual of this tools.

From our test-set, we observed that the overlapping variants are not merged.

#### SigProfilerClusters

We did not find relevant parameters regarding overlapping variants and no reference to overlapping variants in the documentation, paper or manual of this tools.

From our test-set, we observed that the overlapping variants are not merged.

#### Kataegis

We did not find relevant parameters regarding overlapping variants and no reference to overlapping variants in the documentation, paper or manual of this tools.

From our test-set, we observed that the overlapping variants are not merged.

#### 4. What are "overlapping variants"?

Please see comment #3 for an explanation of the algorithm and internal handling. Please see the supplementary rebuttal pdf file that contains mathematical expressions which we use to respond to this important question.

#### 5. Why should they be merged?

We deemed merging overlapping genomic variants necessary as we currently do not implement phasing of alleles or include clonal cancer fractions for detection of kataegis to ease the interpretation and accessibility of katdetectr for a general audience. Therefore, if two overlapping variants would not be merged, they would contain a negative or 0 IMD. This could inflate the detection of kataegis whilst likely reflecting an admixture of clones with mutations on alternate genomes / haplotypes or an altogether complex genomic rearrangement. (line 360)

Please note that any merged records will always contain unique metadata ("revmap") detailing the merged variants, a reference allele of X and an alternative allele of XX. This allows user to manually further investigate these regions.

#### 6. Are there any outcomes of these treatments here?

Within all 1024 synthetic samples constituting a total of 21,299,360 SNVs, 4592 SNVs (0.02%) were merged to a single datapoint.

Within all 507 evaluated WGS samples (Alexandrov et al. 2013) constituting a total of 3,382,751 SNV, no SNVs were merged which likely reflects a pre-filtering step within the initial dataset by the authors.

7. There is a lookup table for chromosome length of UCSC hg19 (in function\_performChangepointDetection.R). Does this tool also support other reference genomes of different species or different versions of human genomes? If so, how can users change this parameter?

The previous version (v1.0.0) as deposited at submission of this article indeed only (erroneously) contained a lookup table for hg19. We previously addressed this reviewer's concern in the following git issue: <https://github.com/ErasmusMC-CCBC/katdetectr/issues/1>

On 26-04-2023, the release branch of BioConductor was updated which includes this update (katdetectr v1.2.0). This updated version of katdetectr contains the argument "refSeq" in detectKataegis() which can be used to specify which human reference genome (by supplying "hg19" or "hg38") should be considered. Additionally, this argument can be used to supply the necessary sequence length for analysis other genomes; allowing for the analysis of additional organisms.

We have also included additional information within the vignette detailing this, please see section: "Analyzing non-standard sequences" in the vignette accompanied with the katdetectr package (v1.2.0): [https://bioconductor.org/packages/devel/bioc/vignettes/katdetectr/inst/doc/General\\_overview.html](https://bioconductor.org/packages/devel/bioc/vignettes/katdetectr/inst/doc/General_overview.html)

8. The authors tested four algorithms of changepoint package for kataegis detection, and found the PELT algorithm outperformed the others. The authors have described the results roughly, could the authors state the reasons in mathematical aspect more detailly? And are these methods recommended in another scenario?

Whilst this is an interesting question, we feel that Killick and Eckley[1,2] have already expertly detailed the various mathematical intricacies of these algorithms, as employed within the changepoint package. These excellent works contain the information concerning; mathematical proofs, computational complexity, definitions of the search algorithms, possible loss functions and their implications, methods for guarding against overfitting, changes in mean, changes in variance, changes in mean and variance, and more examples.

Within our manuscript, we opted to forego this introduction to focus on the empirical performance of these search methods in the context of kataegis detection within WGS data.

[1] R. Killick, P. Fearnhead & I. A. Eckley (2012) Optimal Detection of Changepoints With a Linear Computational Cost, Journal of the American Statistical Association, 107:500, 1590-1598, DOI: 10.1080/01621459.2012.737745

[2] Killick, R., & Eckley, I. A. (2014). changepoint: An R Package for Changepoint Analysis. Journal of Statistical Software, 58(3), 1-19. <https://doi.org/10.18637/jss.v058.i03>

9. I noticed you have added one pseudo IMD in the distance from the last variant to the end of the DNA sequence to make the rates detection in change point analysis equal the mutation rate of the entire chromosome. Why this process is necessary?

Please see the supplementary rebuttal pdf file that contains mathematical expressions which we use to respond to this relevant question.

10. Except for these four algorithms, do you have any plan for implementing other algorithms for this package?

To our understanding, PELT is the current state-of-the-art search algorithm for changepoint analysis. Therefore, have currently employed this as the default algorithm. Nevertheless, we implemented katdetectr in a flexible and open-source manner which allows us or other contributors to easily implement additional search methods when requested. As PELT provided us with overall good results regarding kataegis detection, we do not foresee the immediate usage of alternate methods.

11. In the performance evaluation, you have the same variants files tested with different tools with default parameters. As we know, the tools with PCF algorithms may have parameters of penalty for each discontinuity in the curve. What are these parameters set default in these tools?

Both MafTools and Kataegis mostly employ a Piecewise Constant Fit (PCF) methodology for kataegis detection. To the best of our knowledge, we did not discern a relevant parameter in maftools (`maftools::rainfallPlot()`) which concerns the “penalty for each discontinuity” therefore we cannot comment on this further.

Within the package Kataegis, the `kataegis::kata()` function contains the “gamma” parameter for which the manual states that this sets the “penalty for each discontinuity in the curve” and is by default set to 25 (and was also left default during our performance evaluation).

We have sought to perform all alternative tools utilizing their hard-coded or otherwise suggested default settings as mentioned by the authors in their respective manuscripts and/or manuals to the best of our ability (line 600 - 618). Katdetectr was likewise performed with its defaults settings as described within our manuscript and/or hard-coded default values.

12. Are there any influences on the kataegis detection?

As also mentioned in comment #11, we have sought to perform all alternative tools utilizing their hard-coded or otherwise suggested default settings as mentioned by the authors in their respective manuscripts and/or manuals to the best of our ability (line 621 - 638). Katdetectr was likewise performed with its defaults settings as described within our manuscript and/or hard-coded default values. We have not performed additional parameter sweeps for the alternative packages as we argue that the default settings will be used by the majority of users. We therefore cannot discard that fine-tuning the parameters would have an influence on the current evaluation.

We have added this limitation to the discussion (line 307 - 312).

13. For different tools you have convert the datasets to different formats, i.e., MAF, BED, why do you choose MAF as the input format and how do you keep the input data consistency in all these different formats?

Within katdetectr, we provide functions to import VCF and MAF files or custom VRanges. However, several other evaluated packages were only capable of importing MAF or BED files. Therefore, we converted the variant data into the preferred formats as specified in the respective manuals of each package. Each time, we checked the consistency of the transformed data to exclude possible artefacts during conversion.

All utilized code for the importing and transformation of the data can be found in our GitHub repository:[https://github.com/ErasmusMC-CCBC/evaluation\\_katdetectr/](https://github.com/ErasmusMC-CCBC/evaluation_katdetectr/)

14. For the evaluation scores, could the authors provide raw score of true positive and

	<p>true negative other than TPR and TNR?</p> <p>Supplementary tables 1 and 2 contain the raw data detailing all true positives, false positives, true negatives, and false negatives per package for the synthetic and WGS datasets respectively.</p> <p>15. In addition, the deposited data for performance evaluation is not accessible outside my workplace. And more detailed instructions are necessary for the data. After I loaded the data named parameters_synthetic_data.RData in R, I was lost for deeper looking into the data. When I tried to direct the loaded data to an object, a text of "chr "parameters"" was echoed.</p> <p>To ease further reproducibility of our work, we have implemented a Jupyter (R) Notebook in which the various steps of the comparison can be reproduced in a virtual environment (or within a local R environment when installing the IRkernel package): <a href="https://github.com/ErasmusMC-CCBC/evaluation_katdetectr/blob/main/notebooks/1.EvaluatePackages.ipynb">https://github.com/ErasmusMC-CCBC/evaluation_katdetectr/blob/main/notebooks/1.EvaluatePackages.ipynb</a></p> <p>In addition, this notebook contains a code snippet (using zen4R) which can automatically download all our initial input and generated results directly from Zenodo:<a href="https://dx.doi.org/10.5281/zenodo.6810477">https://dx.doi.org/10.5281/zenodo.6810477</a></p> <p>These downloaded data can then be used in the downstream visualization and performance evaluations code-blocks. We hope this eases the reviewer reproduction of the initial dataset and following steps leading to the (re-)production of all presented figures and tables.</p>
<b>Additional Information:</b>	
<b>Question</b>	<b>Response</b>
Are you submitting this manuscript to a special series or article collection?	No
<p><b>Experimental design and statistics</b></p> <p>Full details of the experimental design and statistical methods used should be given in the Methods section, as detailed in our <a href="#">Minimum Standards Reporting Checklist</a>. Information essential to interpreting the data presented should be made available in the figure legends.</p> <p>Have you included all the information requested in your manuscript?</p>	Yes
<p><b>Resources</b></p> <p>A description of all resources used, including antibodies, cell lines, animals and software tools, with enough information to allow them to be uniquely</p>	Yes

<p>identified, should be included in the Methods section. Authors are strongly encouraged to cite <a href="#">Research Resource Identifiers</a> (RRIDs) for antibodies, model organisms and tools, where possible.</p> <p>Have you included the information requested as detailed in our <a href="#">Minimum Standards Reporting Checklist</a>?</p>	
<p><b>Availability of data and materials</b></p> <p>All datasets and code on which the conclusions of the paper rely must be either included in your submission or deposited in <a href="#">publicly available repositories</a> (where available and ethically appropriate), referencing such data using a unique identifier in the references and in the “Availability of Data and Materials” section of your manuscript.</p> <p>Have you have met the above requirement as detailed in our <a href="#">Minimum Standards Reporting Checklist</a>?</p>	<p>Yes</p>

1 **Katdetectr: An R/Bioconductor package utilizing**  
2 **unsupervised changepoint analysis for robust kataegis**  
3 **detection**

4 Daan M. Hazelaar<sup>1, †</sup> d.hazelaar@erasmusmc.nl  
5 Job van Riet<sup>1-2, †, ^</sup> job.vanriet@dkfz-heidelberg.de  
6 Youri Hoogstrate<sup>3</sup> y.hoogstrate@erasmusmc.nl  
7 Harmen J. G. van de Werken<sup>2,4, \*</sup> h.vandewerken@erasmusmc.nl

8

9 <sup>1</sup>Department of Medical Oncology, Erasmus MC Cancer Institute, Erasmus University Medical Center, Dr.  
10 Molewaterplein 40, 3015 GD, Rotterdam, the Netherlands.

11 <sup>2</sup>Department of Urology, Erasmus MC Cancer Institute, Erasmus University Medical Center, Dr. Molewaterplein  
12 40, 3015 GD, Rotterdam, the Netherlands.

13 <sup>3</sup>Department of Neurology, Erasmus MC Cancer Institute, Erasmus University Medical Center, Dr.  
14 Molewaterplein 40, 3015 GD, Rotterdam, the Netherlands,

15 <sup>4</sup>Department of Immunology, Erasmus MC Cancer Institute, Erasmus University Medical Center, Dr.  
16 Molewaterplein 40, 3015 GD, Rotterdam, the Netherlands.

17 <sup>^</sup>Current Address: Division of AI in Oncology, German Cancer Research Center (DKFZ), Im Neuenheimer Feld  
18 280, 69120, Heidelberg, Germany

19 <sup>†</sup>Shared first-authorship

20 <sup>\*</sup>Corresponding author

21

22 **ORCID iDs:** Daan Mattijn Hazelaar [0000-0002-7513-6813]; Job van Riet  
23 [0000-0001-7767-7923]; Youri Hoogstrate [0000-0003-2166-0676]; Harmen  
24 van de Werken [0000-0002-9794-1477];

25

## 26 **Abstract**

### 27 **Background**

28 Kataegis refers to the occurrence of regional genomic hypermutation in cancer and is a phenomenon that has  
29 been observed in a wide range of malignancies. A kataegis locus constitutes a genomic region with a high  
30 mutation rate, i.e., a higher frequency of closely interspersed somatic variants than the overall mutational  
31 background. It has been shown that kataegis is of biological significance and possibly clinically relevant.  
32 Therefore, an accurate and robust workflow for kataegis detection is paramount.

33

### 34 **Findings**

35 Here we present *Katdetectr*, an open-source R/Bioconductor-based package for the robust yet flexible and fast  
36 detection of kataegis loci in genomic data. In addition, *Katdetectr* houses functionalities to characterize and  
37 visualize kataegis and provides results in a standardized format useful for subsequent analysis. In brief,  
38 *Katdetectr* imports industry-standard formats (MAF, VCF, and VRanges), determines the intermutation  
39 distance of the genomic variants and performs unsupervised changepoint analysis utilizing the Pruned Exact  
40 Linear Time search algorithm followed by kataegis calling according to user-defined parameters.

41

42 We used synthetic data and an *a priori* labeled pan-cancer dataset of Whole Genome Sequenced malignancies  
43 for the performance evaluation of *Katdetectr* and five publicly available kataegis detection packages. Our  
44 performance evaluation shows that *Katdetectr* is robust regarding tumor mutational burden (TMB) and shows  
45 the fastest mean computation time. Additionally, *Katdetectr* reveals the highest accuracy (0.99, 0.99) and  
46 normalized Matthews Correlation Coefficient (0.98, 0.92) of all evaluated tools for both datasets.

47

### 48 **Conclusions**

49 *Katdetectr* is a robust workflow for the detection, characterization, and visualization of kataegis and is  
50 available on Bioconductor: <https://doi.org/doi:10.18129/B9.bioc.katdetectr>

51

52 **Keywords:** Kataegis, R-package, Bioconductor, Changepoint analysis, Cancer.

53

## 54 **Introduction**

55

56 Large-scale next-generation sequencing of malignancies has revealed that a myriad of mutational mechanisms  
57 and mutational rates are at play within even a single tumor genome. Moreover, it has been shown that  
58 mutations can cluster together, i.e., the acquired mutations are found in proximity to one another, much  
59 closer than expected if each base-pair had an equal probability of being mutated. This phenomenon was  
60 termed kataegis and its respective genomic location was termed a kataegis locus [1, 2].

61

62 Kataegis, Greek for thunderstorm or shower, was first observed and visualized in whole genome sequencing  
63 (WGS) data of 21 primary breast cancers [1]. Alexandrov and colleagues, subsequently, detected 873 kataegis  
64 loci in a pan-cancer dataset containing 507 WGS samples from primary malignancies [2].

65

66 Extensive exploration of the etiology of kataegis revealed a significant positive association between kataegis  
67 and two distinct mutational signatures (COSMIC signatures SBS2 and SBS13) both attributed to the APOBEC  
68 enzyme-family [3, 4]. Subsequently, multiple studies confirmed the importance of the APOBEC enzymes in  
69 cancer, showing that APOBEC enzymes are a major cause of mutagenesis, grouped in clusters, dispersed  
70 throughout the cancer genome and in extrachromosomal DNA[5–7]. Additionally, kataegis has been ascribed  
71 in lymphomas to two other mutational signatures (COSMIC signatures SBS84 and SBS85) related to the  
72 APOBEC family member Activation-induced cytidine deaminase (AID) enzyme [8].

73

74 Moreover, the locations of kataegis loci have been associated with locations of somatic structural variant  
75 breakpoints. Kataegis loci have been observed most frequently within the proximity of deletions and complex  
76 rearrangement breakpoints [3, 9]. Furthermore, kataegis can occur within known cancer driver genes including

77 *TP53*, *EGFR* and *BRAF* which are associated with overall survival in some cancer types [5]. However, the clinical  
78 relevance of kataegis remains to be validated and therefore obfuscates kataegis as a clinical biomarker for  
79 prognosis. Moreover, future insight into kataegis etiology and clinical applications requires accurate and  
80 robust detection of kataegis.

81

82 Since the discovery of kataegis, different computational detection tools using genomic variant data have been  
83 developed and are publicly available, including; MafTools [10], ClusteredMutations [11], kataegis [12], SeqKat  
84 [13] and, SigProfilerClusters [14]. These packages employ distinct statistical methods for kataegis detection  
85 and differ in their ease of use and computational feasibility. Therefore, a comparison of their performances is  
86 currently needed.

87

88 Here, we introduce Katdetectr, an R-based Bioconductor package that contains a suite for the detection,  
89 characterization, and visualization of kataegis. Additionally, we have evaluated and compared the performance  
90 of Katdetectr to the five commonly used and publicly available kataegis detection packages.

91

## 92 **Results**

93 The principle of Katdetectr is to assess the variation in the mutation rate of a cancer genome. To achieve this,  
94 Katdetectr starts by importing and preprocessing industry-standard variant calling formats (VCF, MAF,  
95 VRanges) (**Figure 1A**). Next, the Intermutation Distance (IMD) is determined, which denotes the distance  
96 between variants in base-pairs (**Figure 1B**, see Methods). Unsupervised changepoint analysis is performed,  
97 using the IMD as input, which results in detected changepoints. The changepoints, which denote the points at  
98 which the distribution of the IMD changes, are used to segment the genomic sequence. Finally, segments are  
99 annotated and labeled as a putative kataegis locus if a segment fits the user-defined settings: the mean IMD of  
100 the segment  $\leq \text{IMD}_{\text{cutoff}}$  and the number of variants in the segment  $\geq \text{minSizeKataegis}$ . The IMD,  
101 segmentation, and detected kataegis loci can be visualized by Katdetectr in a rainfall plot (**Figure 1C**).

102

103 **Figure 1, Overview of the Katdetectr workflow, Intermutation distance, and rainfall plots.** A) General workflow of Katdetectr from data  
104 import to data visualization represented by arrows. B) The intermutation distance (IMD) is determined for all genomic variants in each

105 chromosome, and rainfall plots are used to visualize the IMDs. Single Nucleotide Variant (SNV), Multi Nucleotide Variant (MNV). C) Rainfall  
106 plot of WGS breast cancers sample PD7049a as interrogated by Katdetectr with  $IMD_{cutoff} = 1,000$  and  $minSizeKataegis = 6$  [2]. Y-axis: IMD,  
107 x-axis: variant ID ordered on genomic location, light blue rectangles: kataegis loci with genomic variants within kataegis loci shown in bold.  
108 The color depicts the mutational type. The vertical lines represent detected changepoints, while black horizontal solid lines show the  
109 mean IMD of each segment.

110

## 111 **Katdetectr search algorithm selection**

112 To optimize Katdetectr for kataegis detection, we generated a synthetic dataset to test four changepoint  
113 search algorithms, namely; Pruned Exact Linear Time (PELT) [15], Binary Segmentation (BinSeg) [15], Segment  
114 Neighbourhoods (SegNeigh) [17], and At Most One Change (AMOC). The synthetic dataset contains 1024  
115 samples with a varying number of kataegis loci and Tumor Mutational Burden (TMB) (see Methods). All  
116 variants in this dataset were binary labeled for kataegis, as a variant either lies within a kataegis locus (TRUE)  
117 or not (FALSE). This dataset was considered ground truth and was used for computing performance metrics.  
118 We analyzed the synthetic dataset separately for each search algorithm showing that the PELT algorithm  
119 outperformed the alternatives (**Supplementary table 1, supplementary figure 1, 2**). Therefore, we set PELT as  
120 the default search algorithm in Katdetectr.

121

## 122 **Performance evaluation**

123 We utilized the synthetic dataset to evaluate the performances of Katdetectr and five publicly available  
124 kataegis detection packages: MafTools, ClusteredMutations, Kataegis, SeqKat, and, SigProfilerClusters (**Table 1,**  
125 **supplementary table 1**). Katdetectr revealed the highest overall accuracy (0.99), normalized Matthews  
126 Correlation Coefficient (nMCC: 0.98), and F1 score (0.97), whereas ClusteredMutations showed the highest  
127 True Positive Rate (TPR: 0.99) and Kataegis showed the highest True Negative Rate (TNR: 0.99). Most packages  
128 showed a high nMCC for samples with a TMB ranging from 0.1 - 50. However, the performance of all packages  
129 dropped for samples with a  $TMB \geq 100$  (**Figure 2A**). More specifically, for Katdetectr and Kataegis, this is due to  
130 an increase in false negatives. For SeqKat, MafTools, ClusteredMutations, and SigProfilerClusters, this  
131 performance drop is due to an increase in false positives in samples with a TMB of 100 and 500  
132 (**Supplementary figure 1**).

133

134 Next to the synthetic dataset, we evaluated the performance of the kataegis detection packages on a dataset  
 135 containing 507 *a priori* labeled Whole Genome Sequenced (WGS) samples from Alexandrov *et al.* (see  
 136 Methods) [2]. Katdetectr revealed the highest overall accuracy (0.99), nMCC (0.92), and F1 score (0.83),  
 137 whereas ClusteredMutations showed the highest TPR (0.99) and SigProfilerClusters showed the highest TNR  
 138 (0.99) (**Table 1, Supplementary figure 1**). Katdetectr, ClusteredMutations, and MafTools showed a high nMCC  
 139 (>0.92) on the samples with a low or middle TMB. However, the performance of all packages drops for samples  
 140 with a TMB >10 (n = 20) (**figure 2A**). This is due to an increase in false negatives by Kataegis and SeqKat and  
 141 false positives by Katdetectr, MafTools, ClusteredMutations, and SigProfilerClusters.

142

143 **Summary and performance of kataegis detection packages.**

Package	Reference	Available on	Language	Method	Synthetic dataset					WGS dataset				
					Accuracy	nMCC	F1	TPR	TNR	Accuracy	nMCC	F1	TPR	TNR
Katdetectr	Hazelaar, van Riet et al., 2023	Bioconductor	R	Changepoint analysis (PELT)	<u>0.99</u>	<u>0.98</u>	<u>0.97</u>	0.94	0.99	<u>0.99</u>	<u>0.92</u>	<u>0.83</u>	0.91	0.99
SeqKat	Taylor et al., 2013	CRAN	R	Sliding window / exact binomial test	0.84	0.54	0.02	0.93	0.84	0.99	0.85	0.69	0.59	0.99
MafTools	Mayakonda et al., 2018	Bioconductor	R	Sliding window / PCF	0.74	0.53	0.01	0.96	0.74	0.99	0.85	0.66	0.93	0.99
SigProfilerClusters	Bergstrom, Kundu, et al., 2022	Github	Python	Model sample specific IMD cutoff	0.65	0.52	0.01	0.88	0.65	0.99	0.84	0.68	0.66	<u>0.99</u>
ClusteredMutations	Lora, 2016	CRAN	R	Anti-Robinson matrix	0.70	0.53	0.01	<u>0.99</u>	0.74	0.99	0.83	0.61	<u>0.99</u>	0.99
Kataegis	Lin et al., 2021	Github	R	PCF	0.99	0.80	0.52	0.36	<u>0.99</u>	0.99	0.56	0.03	0.02	0.99

144

145 **Table 1.** Summary information of all evaluated kataegis detection packages and their respective performance metrics regarding kataegis  
 146 classification on 1,024 synthetic samples and 507 *a priori* labeled Whole Genome Sequenced (WGS) samples. Accuracy, normalized  
 147 Matthews Correlation Coefficient (nMCC), F1 score, True Positive Rate (TPR) and True Negative Rate (TNR), Pruned Exact Linear Time  
 148 (PELT), Piecewise Constant Fit (PCF), Intermutation Distance (IMD).

149

150 We visualized the concordance regarding per sample kataegis classification and kataegis locus between  
 151 Katdetectr, SigProfilerClusters, ClusteredMutations, MafTools, and the original authors of the WGS dataset:  
 152 Alexandrov *et al.*, 2013 (**Figure 2B**). In total, 451 kataegis loci were detected in 127 WGS samples by all the  
 153 packages and the original publication. Interestingly, Katdetectr, SigProfilerClusters, ClusteredMutations, and  
 154 MafTools concordantly detected 102 previously unannotated kataegis loci within the original publication.

155

156 The runtimes of all packages were recorded to give insight into the computational feasibility of these packages.  
 157 Katdetectr showed the lowest mean runtime on both the synthetic and the WGS datasets (**figure 2C**).

158

159 **Figure 2. Performance evaluation of kataegis detection tools.** A) The normalized Matthews Correlation Coefficient (nMCC) per package  
 160 and Tumor Mutational Burden (TMB) class is depicted by individual data points connected with a dashed line (colored per package). B)  
 161 Venn diagrams showing the concordance between Katdetectr, SigProfilerClusters, MafTools, ClusteredMutations, and Alexandrov et al.

162 regarding kataegis classification per sample (i.e., does a sample contain one or more kataegis loci) and per kataegis loci (i.e., does a  
163 detected kataegis locus overlap with a kataegis locus detected by another package). C) Boxplots with individual data points represent the  
164 per sample runtimes of kataegis detection packages on the synthetic and Whole Genome Sequence datasets. Boxplots were sorted in  
165 ascending order based on mean runtime (depicted in the text below the boxplot). Y-axis is  $\log_{10}$ -scaled. Boxplots depict the Inter Quartile  
166 Range, with the median as a black horizontal line.

167

## 168 **Katdetectr examples with different TMBs**

169 We highlight four samples from the datasets that illustrate how Katdetectr accurately detects kataegis loci  
170 regardless of the TMB of the respective sample (**Figure 3**). The synthetic sample 124625\_1\_50\_100 (TMB: 500)  
171 harbors one kataegis locus, containing 57 variants, which is detected by Katdetectr (**Figure 3A**). This kataegis  
172 locus is also detected by SeqKat, MafTools, ClusteredMutations, and SigProfilerClusters, in addition to  
173 numerous false positives. The package Kataegis did not detect any kataegis loci in this synthetic sample.

174

175 In lung adenocarcinoma sample LUAD-E01014 (TMB: 7.6), Katdetectr detected 37 kataegis loci containing 449  
176 variants (**Figure 3B**). MafTools, ClusteredMutations, and SeqKat detected similar kataegis loci in this sample,  
177 whereas Kataegis and SigProfilerClusters did not detect any kataegis loci in this sample. In breast cancer  
178 sample PD7207a (TMB: 0.8), two kataegis loci were detected by Katdetectr MafTools, ClusteredMutations, and  
179 SigProfilerClusters (**Figure 3C**). Kataegis and SeqKat did not detect any kataegis loci in this sample. Lastly, in the  
180 breast cancer sample PD4086a (TMB: 0.6), one kataegis locus was detected by all packages except for Kataegis  
181 (**Figure 3D**).

182

183 **Figure 3. Rainfall plots constructed by Katdetectr and confusion matrices, accuracy, and nMCC for four samples.** A) Synthetic sample  
184 124625\_1\_50\_100 with Tumor Mutational Burden (TMB): 500, B) Lung adenocarcinoma Whole Genome Sequenced (WGS) sample LUAD-  
185 E01014 with TMB: 7.6. C) Breast cancer WGS sample PD7207a with TMB: 2.5. D) Breast cancer WGS sample PD4086a with TMB: 0.62. The  
186 WGS samples were collected and labeled for kataegis by Alexandrov *et al.*; their results were used as ground truth to construct the  
187 confusion matrices and performance metrics [2]. Rainfall plot: Y-axis: IMD, x-axis: variant ID ordered on genomic location, light blue  
188 rectangles: kataegis loci with genomic variants within kataegis loci shown in bold. The color depicts the mutational type. The vertical lines  
189 represent detected changepoints, while black horizontal solid lines show the mean IMD of each segment. Confusion matrix: True Positive  
190 (TP), False Positive (FP), True Negative (TN), False Negative (FN), Accuracy, and normalized Matthews Correlation Coefficient (nMCC).

191

## 192 **Discussion**

193 Here, we described Katdetectr, an R/Bioconductor package for the detection, characterization, and  
194 visualization of kataegis in genomic variant data by utilizing unsupervised changepoint analysis.

195

196 First, we tested four search algorithms for changepoint analysis, which revealed that the PELT [15] algorithm  
197 outperformed the BinSeg [16], SegNeigh [17], and AMOC algorithms both in terms of prediction accuracy and  
198 computational feasibility. The BinSeg algorithm performed reasonably well, however, it underfitted the data,  
199 which resulted in many false negatives. The SegNeigh algorithm performed well on samples with a TMB < 5;  
200 however, this algorithm is computationally expensive, as it scales exponentially with the size of the data, and  
201 cannot reasonably be used for the analysis of samples with a TMB > 10. Unsurprisingly, the AMOC (at most  
202 one change) algorithm cannot detect kataegis as a kataegis locus is generally defined by two changepoints.

203

204 Besides testing search algorithms, we benchmarked Katdetectr using PELT and five publicly available kataegis  
205 detection packages which were recently published and used for supporting kataegis research [2, 5, 14, 15].  
206 Since no consensus benchmark was available, we aimed to get insight into the performance of these tools. The  
207 complexity of kataegis detection is to separate genomic regions of higher-than-expected mutational density  
208 from the background of somatic mutations. Therefore, we argued that generating a synthetic dataset  
209 containing samples of varying TMB (0.1-500), would provide a good measure for algorithmic solvability of the  
210 kataegis detection problem. Benchmarking on this synthetic dataset revealed that the accuracy of kataegis  
211 detection for all evaluated packages drops when the TMB increases. Performance evaluation per TMB-binned  
212 class revealed that Katdetectr is on par with alternative packages for samples with low or middle TMB.  
213 However, in contrast to alternative packages, Katdetectr remained robust when analyzing samples with a high  
214 TMB. This could be an important feature when analyzing late-stage (metastatic) malignancies or malignancies  
215 with a known predisposition of acquiring many somatic mutations such as skin or lung malignancies [20].  
216 Additionally, the computation times of Katdetectr are feasible for samples with a TMB ranging from 0.1 to 500  
217 as PELT scales linearly with the size of the data [15]. This shows that kataegis detection using Katdetectr is  
218 feasible on reasonably modern computer hardware.

219

220 The presented performance evaluation depends on the truth labels provided by the datasets. Both the  
221 synthetic and the WGS dataset have their limitations. We constructed the synthetic dataset by modeling  
222 mutations on a genome as a Bernoulli process, which is a common approach for modeling events that occur in  
223 a sequence. However, we did not incorporate prior biological knowledge in the synthetic dataset generation.  
224 Both SeqKat and SigProfilerClusters incorporate biological assumptions regarding kataegis, e.g., mutation  
225 context, which possibly negatively influenced their performance regarding the synthetic dataset. Additionally,  
226 the distance between events generated by a Bernoulli process is a geometric random variable. For a large  $n$ ,  
227 which is the case for a human genome, a geometric random variable approximates an exponential random  
228 variable. Since we constrain Katdetectr to only fit exponential distributions it is unsurprising that Katdetectr  
229 performs well on the synthetic dataset. Nevertheless, MafTools, ClusteredMutations, SeqKat, and  
230 SigProfilerClusters are less robust when analyzing the synthetic samples with a TMB of 100 and 500 as they  
231 classify many false positives kataegis loci.

232

233 In addition to the synthetic dataset, we used the *a priori* labeled pan-cancer WGS dataset from the  
234 groundbreaking work of Alexandrov *et al.* to evaluate the kataegis detection tools [2]. However, the field of  
235 kataegis has grown and evolved since the publication of this dataset. Therefore, we want to emphasize that  
236 this dataset should not be considered an unequivocal truth, and the performance metrics should not be taken  
237 at face value. The annotation of this dataset likely contains several false positives and false negatives; as  
238 highlighted by the concordant discovery of 102 additional kataegis loci by several packages. Nevertheless, we  
239 believe that the current benchmarking results give insight into the behavior of the evaluated packages  
240 regarding kataegis classification in samples with varying TMB. Additionally, the dataset published by  
241 Alexandrov and the predictions by all tools evaluated here are publicly available which facilitates  
242 benchmarking of future endeavors regarding kataegis loci detection methods.

243

244 Our benchmarking showed that, for the WGS dataset, Katdetectr, MafTools, ClusteredMutations, and,  
245 SigProfilerClusters have a high concordance in classifying a whole sample as kataegis positive or negative.  
246 However, when concerning distinct kataegis loci, we observed more differences. ClusteredMutations reported  
247 the overall largest number of loci ( $n = 2,360$ ), indicating it has the highest sensitivity. Conversely, kataegis ( $n =$   
248 8) and SeqKat ( $n = 528$ ) reported the overall smallest number of loci which we deem too small based on visual

249 inspection. The third smallest number of kataegis loci is reported by SigProfilerClusters (n = 764), indicating it  
250 has the highest specificity. Katdetectr appears to balance sensitivity and specificity as it only detects kataegis  
251 loci detected by one or more alternative packages (n = 1,050).

252

253 We have sought to test the performance of all alternative tools utilizing their hard-coded or otherwise  
254 suggested default settings as mentioned by the authors in their respective manuscripts or manuals. Katdetectr  
255 was likewise performed with its default settings as described within this manuscript. We have not performed  
256 additional parameter sweeps for the alternative packages as we argue that the default settings will be used by  
257 the majority of users. We therefore cannot discard that fine-tuning the parameters would have had an  
258 influence on our performance evaluation.

259

260 Kataegis is the most commonly used term for local hypermutations and has historically been defined as a  
261 cluster of at least six variants, of which the mean IMD is less or equal to 1000 base pairs [1, 16]. However, this  
262 definition has been altered recently, making the formal definition of kataegis ambiguous [2, 4, 5, 14]. For  
263 instance, another type of clustered mutations is called Omikli, which refers to clusters smaller than kataegis,  
264 generally containing three or four variants [7]. Although different types of clustered variants can be detected  
265 using Katdetectr by supplying the correct parameters, we only evaluated Katdetectr for the detection of  
266 kataegis.

267

268 We made Katdetectr publicly available on the Bioconductor platform, which requires peer-reviewed open-  
269 source software and high standards regarding development, documentation, and unit testing. Furthermore,  
270 Bioconductor ensures reliability and operability on common operating systems (Windows, macOS, and Linux).  
271 We designed Katdetectr to fit well in the Bioconductor ecosystem by incorporating common Bioconductor  
272 object classes. This allows Katdetectr to be used reciprocally with the plethora of statistical software packages  
273 available in Bioconductor for preprocessing and subsequent analysis. Lastly, we implemented Katdetectr  
274 flexibly, allowing Katdetectr to be used in an ad hoc manner for quick assessment of clustered variants and  
275 extensive research of the mutation rates across a tumor genome.

276

## 277 Conclusion

278 Katdetectr is a free, open-source R package available on Bioconductor that contains a suite for the detection,  
279 characterization, and visualization of kataegis. Katdetectr employs the PELT search algorithm for unsupervised  
280 changepoint analysis, resulting in robust and fast kataegis detection. Additionally, Katdetectr has been  
281 implemented in a flexible manner which allows Katdetectr to expand in the field of kataegis. Katdetectr is  
282 available on Bioconductor[21] and on GitHub[22].

283

## 284 Methods

### 285 Implementation Katdetectr

286 Katdetectr (v1.2.0, git commit 5a6e5d04109eb082cbea040049dca34237b6c8f5) was developed in the R  
287 statistical programming language (v4.2.0) [23]. Katdetectr imports genomic variants through generic,  
288 standardized file formats for variant calling: MAF, VCF, or Bioconductor-standard VRanges objects. Within  
289 Katdetectr, the imported variants are pre-processed such that, per chromosome, all variants (all rows in  
290 variant file; incl. InDels or structural variations) are sorted in ascending order based on their genomic position.  
291 Overlapping variants are merged into a single record as phasing and clonality are not considered by katdetectr.  
292 Following, per *chromosome<sub>j</sub>*, the intermutation distance ( $IMD_{i,j}$ ) of each *variant<sub>i,j</sub>* and its closest upstream  
293 *variant<sub>i-1,j</sub>* is calculated according to;

294

$$295 \quad IMD_{i,j} = \begin{cases} i = 1 & s_{i,j} \\ i > 1 & s_{i,j} - s_{i-1,j} \end{cases} \quad i = \{1, 2, \dots, k_j\}$$

296 *Equation 1*

297 With  $i$  as the variant number,  $j$  as the chromosome number,  $s$  as the genomic location of the first base-pair of  
298 a *variant<sub>i,j</sub>* and  $k_j$  as the total number of variants in *chromosome<sub>j</sub>* (**Figure 1B**). Additionally, for each  
299 *chromosome<sub>j</sub>* one pseudo IMD,  $IMD_{p,j}$ , is added such that;

$$300 \quad n_j = IMD_{p,j} + \sum_{i=1}^{k_j} IMD_{i,j}$$

301 *Equation 2*

302 With  $n_j$  as the total number of base-pairs in *chromosome<sub>j</sub>*

303 Katdetectr aims to identify genomic regions characterized by specific mutation rates. An unsupervised  
304 technique called changepoint analysis is performed per chromosome on the IMDs to assess the variability in  
305 mutation rate across each chromosome. Changepoint analysis refers to the process of detecting points in a  
306 sequence of observations where the statistical properties of the sequence significantly change. Subsequently,  
307 the detected changepoints are used to segment the input sequence into segments. For a detailed description  
308 of the changepoint analysis, see the work of Killick, Fearnhead, and Eckley [15]

309 We implemented the `cpt.meanvar()` function from the commonly used R changepoint package (v2.2.3) in  
310 Katdetectr for the unsupervised segmentation of IMDs, as detailed by [11, 20, 21]. We set the following  
311 parameters settings; method: Pruned Exact Linear Time (PELT), minimal segment length: 2, test statistic:  
312 Exponential, and penalty: Bayesian Information Criterion (BIC), as default settings in Katdetectr.

313

314 After changepoint analysis, each segment is annotated with its respective genomic start and end positions, its  
315 mean IMD, and the total number of included variants. Since we use an exponential distribution as the test  
316 statistic in changepoint analysis, each segment has a corresponding rate parameter of the fitted exponential  
317 distribution. Whereas each segment is annotated with its corresponding mutation rate, the mutation rate of  
318 an entire sample can be expressed as the weighted arithmetic mean of the mutation rate of the segments;

319

$$320 \quad \lambda_t = \frac{k_t}{n_t} = \sum_{s=1}^m \frac{\lambda_s n_s}{n_t}$$

321 *Equation 3*

322

323 With  $\lambda_t$  as the mutation rate of the entire sample,  $k_t$  as the total number of variants present in the sample,  $n_t$   
324 as the total number of base pairs in the genome,  $m$  as the total number of segments in the sample, and  $\lambda_s$  and  
325  $n_s$  as the mutation rate and the number of base-pairs in *segment<sub>s</sub>*

326

327 To call a segment a putative kataegis locus, it has to adhere to two user-defined parameters: the maximum  
328 mean IMD of the segment (*IMDcutoff*) and the minimum number of included variants (*minSizeKataegis*). These

329 parameters can be provided as static integer values or as a custom R function determining the IMD cutoff for  
 330 each segment. For example, the following function for annotation of kataegis events, as was used by the  
 331 ICGC/TCGA Pan-Cancer Analysis of Whole Genomes Consortium, can be easily implemented in Katdetectr [3]:  
 332

$$333 \quad \text{IMDcutoff}_s \leq \frac{-\log\left(1 - \sqrt[k_s-1]{\frac{0.01}{L_s}}\right)}{\lambda_{med}}$$

334

335 with;  $[\text{IMDcutoff}] = 1000$

336 *Equation 4*

338

337

339 With  $\text{IMDcutoff}_s$  as the IMD cut-off value,  $k_s$  as the number of mutations and  $L_s$  as the length of  $\text{segment}_s$   
 340 in base-pairs. For this function the rate of the whole sample is modeled assuming an exponential distribution  
 341 with;

342

$$343 \quad \lambda_{med} = \frac{\log(2)}{\text{median}(\text{IMD})}$$

344 *Equation 5*

345 Henceforth, all segments satisfying these user-specified parameters are considered putative kataegis loci and  
 346 stored appropriately. Two or more adjacent kataegis loci are merged and stored as a single record.

347

348 The output of Katdetectr consists of an S4 object of class “KatDetect” which stores all relevant information  
 349 regarding kataegis detection and characterization. A KatDetect object contains four slots: 1) the putative  
 350 kataegis loci (Granges), 2) the detected segments (Granges), 3) the inputted genomic variants with annotation  
 351 (Vranges), and 4) the parameters settings (List). These data objects can be accessed using accessor functions.

352

353 In addition, we implemented three methods for the KatDetect class, *summary*, *show*, and *rainfallPlot*. In  
 354 concordance with R standards, the *summary* function prints a synopsis of the performed analysis, including the

355 number of detected kataegis loci; and the number of variants inside a kataegis loci. The *show* function displays  
356 information regarding the S4 class and the synopsis.

357

358 The method *rainfallPlot* is a function for generating rainfall plots. These rainfall plots display the genomic  
359 ordered IMDs (from all genomic variants) within a sample and highlight putative kataegis loci and associated  
360 genomic variants. This function has additional arguments: *showSequence*, which allow the user to display  
361 specific chromosomes, and *showSegmentation*, for displaying the changepoints and the mean IMD of all  
362 segments.

363

364 For additional examples and more hands-on technical instructions, we refer to the accompanying vignette  
365 (**Supplemental vignette**) or the online Bioconductor repository[21].

366

### 367 **Performance evaluation**

368 As multiple packages for kataegis detection are publicly available, we compared Katdetectr against MafTools  
369 (v2.13.0), ClusteredMutations (v1.0.1), kataegis (v0.99.2), SeqKat (v0.0.8) and, SigProfilerClusters (v1.0.11) [6-  
370 10]. For benchmarking, we used an in-house generated synthetic dataset and an *a priori* labeled pan-cancer  
371 dataset of whole genome sequenced malignancies. As not all evaluated packages accepted InDels

372

373 We used the following definition of kataegis as postulated by Alexandrov and colleagues: a kataegis locus is 1)  
374 a continuous segment harboring  $\geq 6$  variants and 2) the captured IMDs within the segment have a mean IMD of  
375  $\leq 1000$  bp [2]. To quantify and compare performances, the task of kataegis detection was reduced to a binary  
376 classification problem. The task of the kataegis detection packages was to correctly label each variant for  
377 kataegis, i.e., whether or not a genomic variant lies within a kataegis locus.

378

### 379 **Performance metrics**

380 Only a small fraction of all observed variants is located within kataegis loci, this results in a large class  
381 imbalance which renders the interpretation of performance metrics, such as accuracy, F1, TPR, and TNR,  
382 counterintuitive and possibly unrepresentative (**Equation 3**). Therefore, the normalized Matthews Correlation

383 Coefficient (nMCC) was used as the primary metric for performance evaluation. The nMCC considers  
384 performance proportionally to both the size of positive and negative elements in a dataset [26].

$$385 \quad Accuracy = \frac{TP + TN}{TP + FP + TN + FN}$$

386

$$387 \quad MCC = \frac{TP \cdot TN - FP \cdot FN}{\sqrt{(TP + FP) \cdot (TP + FN) \cdot (TN + FP) \cdot (TN + FN)}}$$

388

$$389 \quad nMCC = \frac{MCC + 1}{2}$$

390

$$391 \quad F1 = \frac{TP}{TP + \frac{1}{2}(FP + FN)}$$

392

$$393 \quad TPR = \frac{TP}{TP + FN}$$

394

$$395 \quad TNR = \frac{TN}{TN + FP}$$

396

397 *Equation 6. Performance metrics. Accuracy, Matthews Correlation Coefficient (MCC), normalized Matthews Correlation*  
398 *Coefficient (nMCC), F1 score, True Positive Rate (TPR), and True Negative Rate (TNR).*

399 *True Positive (TP): Predicted: variant in kataegis locus. Truth set: variant in kataegis locus.*

400 *False Positive (FP): Predicted: variant in kataegis locus. Truth set: variant not in kataegis locus.*

401 *True Negative (TN): Predicted: variant not in kataegis locus. Truth set: variant not in kataegis locus.*

402 *False Negative (FN): Predicted: variant not in kataegis locus. Truth set: variant in kataegis locus.*

403

404 We utilized Venn diagrams to display the concordance of the kataegis detection packages. We showed in  
405 which samples the packages detected one or more kataegis loci and which kataegis loci were detected by the  
406 packages. Two packages are said to detect the same kataegis locus if the genomic locations of their respective  
407 kataegis locus overlap by at least one base pair.

408

409 To give insight into the package's computation time, the packages runtime performance was recorded using  
410 the `proc.time()` function from the base R package. All packages and comparisons were run on the same  
411 server utilizing an AMD EPYC 7742 64-Core Processor. The packages `Katdetectr` and `SigProfilerClusters`  
412 contained options for parallel processing and used at most four cores per sample during the analyses. All other  
413 packages used a single processing core per sample.

414

415 All scripts necessary for running and visualizing the performance evaluation of all evaluated packages are  
416 available on GitHub[22]. All data used for the performance evaluation is available at Zenodo[27].

417

### 418 **Synthetic data generation**

419 The synthetic dataset was generated using the `generateSyntheticData()` function within the  
420 `Katdetectr` package. Mutations were randomly sampled on a reference genome such that each base has an  
421 equal probability,  $p$ , of being mutated (except for N bases for which  $p = 0$ ). This reduces the occurrence of  
422 mutations on the reference genome to a sequence of  $X_1, X_2, \dots, X_n$ , independent Bernoulli trials,  $X_i$ , i.e., a  
423 Bernoulli process, where;

424

$$425 \quad \mathbf{P}(X_i = 1) = \mathbf{P}(\text{Mutation at } i\text{th base}) = p$$

$$426 \quad \mathbf{P}(X_i = 0) = \mathbf{P}(\text{No mutation at } i\text{th base}) = 1 - p$$

427 *Equation 7*

428 with probability mass function (PMF), expectation and variance:

429

$$430 \quad p_s(k) = \binom{n}{k} p^k (1 - p)^{n-k}, \quad k = 0, 1, \dots, n$$

431

$$432 \quad \mathbf{E}(S) = np$$

433

$$434 \quad \text{var}(S) = np(1 - p)$$

435 *Equation 8*

436 with  $p$  as the probability of success (i.e., mutation),  $n$  as the number of independent trials (i.e., length of the  
 437 genome in base pairs), and  $k$  as the number of successes (i.e., number of occurred mutations). The IMD now  
 438 reduces to geometric random variable  $T$ ; with PMF, expectation, and variance:

439

$$440 \quad p_T(t) = (1 - p)^{-1}p$$

441

$$442 \quad \mathbf{E}(T) = \frac{1}{p}$$

443

$$444 \quad \text{var}(T) = \frac{1 - p}{p^2}$$

445 *Equation 9*

446 The genomic start location of a kataegis locus was sampled as an independent Bernoulli trial. The genomic end  
 447 location of a kataegis locus was calculated using:

448

$$449 \quad \text{end}_i = \text{start}_i + \mathbf{E}(T)_i(k_i + 1) - 1$$

450 *Equation 10*

## 451 **Synthetic dataset description**

452 The synthetic data consists of 1,024 samples with a total of 21,299,360 SNVs (**Table 2**). All mutations were  
 453 generated on chromosome 1 on the human reference genome hg19. These samples were generated such that  
 454 8 different TMB classes (0.1, 0.5, 1, 5, 10, 50, 100, 500) were considered.

455

$$456 \quad TMB = \frac{\text{total number of variants in sample}}{\text{length of genome in bp}} * 10^6$$

457 *Equation 11*

458 For each TMB class, a sample was generated for all combinations of the following parameters: the number of  
 459 kataegis loci (1, 2, 3, 5); the number of variants within each kataegis loci (6, 10, 25, 50); and the expected IMD  
 460 of the variants in kataegis loci (100, 250, 500, 750). This resulted in 64 kataegis samples per TMB class. To

461 balance the dataset, 64 samples without kataegis loci were generated for each TMB class. The synthetic  
 462 dataset contained 1,232 kataegis loci and 33,245 variants within kataegis loci.

463

464 **Descriptive statistics of synthetic dataset**

TMB class (no. of background mutations)	No. Samples (with kataegis)	No. Kataegis loci	No. Variants in kataegis loci
0.1 (25)	128 (64)	176	4,005
0.5 (125)	128 (64)	176	4,,006
1 (249)	128 (64)	176	4006
5 (1,246)	128 (64)	176	4,014
10 (2,493)	128 (64)	176	4,,029
50 (12,463)	128 (64)	176	4077
100 (24,925)	128 (64)	176	4,183
500 (124,625)	128 (64)	176	4,925

465 **Table 2.** Showing per Tumor Mutational Burden (TMB) class: TMB, number of generated background mutations per sample, the total  
 466 number of samples, total number of samples with kataegis, total number of kataegis loci, and total number of variants within a kataegis  
 467 loci of 1024 synthetic samples.

468

469 **Whole Genome Sequence (WGS) dataset description**

470 The WGS dataset (as used in this study; **table 3**) is publicly available in .txt format[2]. This dataset contained  
 471 7,042 primary cancer samples from 30 different tissues; of which 507 originate from whole genome  
 472 sequencing (WGS) and 6,535 from whole exome sequencing (WES). Only the WGS samples ( $n = 507$ ) were  
 473 originally labeled using a Piece-Wise Constant Fit (PCF) model and manually curated for kataegis presence (or  
 474 absence) by the original study. Only the respective WGS samples, with a total of 3,382,751 SNVs, were re-  
 475 interrogated within our performance evaluation. Additionally, we binned this dataset into three TMB classes  
 476 (low:  $TMB < 0.1$ , middle:  $0.1 \geq TMB < 10$ , high:  $TMB \geq 10$ ) and filtered it such that it only contained single  
 477 nucleotide variants (SNVs).

478

479 **Descriptive statistics of WGS dataset.**

TMB class	# Samples (with kataegis)	# Kataegis loci	# Variants in kataegis loci
Low: TMB < 0.1	301(45)	93	946
Middle: $0.1 \geq$ TMB < 10	186 (89)	444	5,058
High: TMB $\geq$ 10	20(18)	336	3,107

480 **Table 2.** Showing per Tumor Mutational Burden (TMB) class: TMB range, the total number of samples, total number of samples with  
481 kataegis, total number of kataegis loci, and total number of variants within a kataegis loci of 507 Whole Genome Sequenced (WGS)  
482 samples labeled by Alexandrov *et al.* [1].

483

### 484 **Pre-processing and parameter settings of alternative kataegis detection packages**

485 Both the synthetic and the Alexandrov *et al.* datasets were converted to MAF format for use in MafTools [10]  
486 ClusteredMutations [11], and kataegis [12] and to BED format for use in SeqKat [13]. All other parameter  
487 settings for MafTools, kataegis, ClusteredMutations, and SeqKat were set to the default values as specified in  
488 their respective manuals and vignettes.

489

490 For SigProfilerClusters [14] both the synthetic and the Alexandrov *et al.* datasets were converted to a .txt file  
491 with column names as specified in the manual of SigProfilerClusters. We set the following parameters for  
492 SigProfilerSimulator(): genome="GRCh37", contexts = ['288'], simulations=100, overlap=True. For subsequent  
493 cluster detection, we set the following parameters for SigProfilerClusters.analysis(): genome="GRCh37",  
494 contexts="96", simContext=["288"], analysis="all", sortSims=True, subClassify=True, correction=True,  
495 calculateIMD=True, max\_cpu=4, includedVAFs=False.

496

497 From the output of SigProfilerClusters we selected the class 2 (kataegis) clusters for further analysis. The  
498 definition of kataegis used by SigProfilerClusters differs from the one used in our performance evaluation.  
499 SigProfilerClusters defines kataegis as a cluster of  $\geq 4$  genomic variants of which the mean IMD is statistically  
500 different from the sample specific IMD cut-off. To include SigProfilerClusters in our performance evaluation we  
501 only selected clusters detected by SigProfilerClusters that fit the definition of kataegis we used for the  
502 performance evaluation, i.e., a kataegis locus contains  $\geq 6$  genomic variants with a mean IMD  $\leq 1,000$  bp.

## 503 **Funding**

504 This research received funding from the Daniel den Hoed Fonds - Cancer Computational Biology Center (DDHF-  
505 CCBC) grant.

506

## 507 **Competing interests**

508 None declared.

509

## 510 **Data availability**

511 All data used in the performance evaluation can be found on Zenodo[27]. All supporting data and materials  
512 are available in the *GigaScience* GigaDB database [28].

513

## 514 **List of abbreviations**

515 AMOC: At Most One Change, bp: base-pair, BinSeg: Binary Segmentation, IMD: Intermutation Distance, MAF:  
516 Mutation Annotation Format, MNV: Multi Nucleotide Variant, nMCC: normalized Matthews Correlation  
517 Coefficient, PCF: Piecewise Constant Fit, PELT: Pruned Exact Linear Time, SNV: Single Nucleotide Variant,  
518 SegNeigh: Segment Neighbourhoods, TMB: Tumor Mutational Burden, TNR: True Negative Rate, TPR: True  
519 Positive Rate, VCF: Variant Calling Format, WES: Whole Exome Sequencing, WGS: Whole Genome Sequencing.

## 520 **Availability of supporting source code and requirements**

521 • Project name: **Katdetectr**

522 • RRID: **SCR\_023506**

523 • BiotoolsID: **katdetectr**

524 • Workflowhub: [10.48546/workflowhub.workflow.463.1](https://www.workflowhub.eu/workflows/10.48546/workflowhub.workflow.463.1)

525 • Project home page:

526 • <https://bioconductor.org/packages/release/bioc/html/katdetectr.html>

- 527 • <https://github.com/ErasmusMC-CCBC/katdetectr>
- 528 • Operating system(s): Platform independent
- 529 • Programming language: R (>= 4.2)
- 530 • Other requirements:
- 531 BiocParallel (>= 1.26.2), changepoint (>=2.2.3), checkmate (>= 2.0.0), dplyr (>= 1.0.8),
- 532 GenomicRanges (>= 1.44.0), GenomelInfoDb (>= 1.28.4), IRanges (>=2.26.0), maftools (>= 2.10.5),
- 533 methods (>= 4.1.3), rlang (>= 1.0.2), S4Vectors (>= 0.30.2), tibble (>= 3.1.6), VariantAnnotation (>=
- 534 1.38.0), Biobase (>= 2.54.0), Rdpack (>= 2.3.1), ggplot2 (>= 3.3.5), tidyr (>= 1.2.0), BSgenome (>=
- 535 1.62.0), ggtext (>= 0.1.1), BSgenome.Hsapiens.UCSC.hg19 (>= 1.4.3), BSgenome.Hsapiens.UCSC.hg38
- 536 (>= 1.4.4), plyranges (>= 1.17.0)
- 537 • License: GPL-3
- 538
- 539 • Project name: **Evaluation of Katdetectr and alternative kataegis detection packages**
- 540 • Workflowhub: [10.48546/workflowhub.workflow.500.1](https://www.workflowhub.eu/workflows/10.48546/workflowhub.workflow.500.1)
- 541 • Project home page: [https://github.com/ErasmusMC-CCBC/evaluation\\_katdetectr](https://github.com/ErasmusMC-CCBC/evaluation_katdetectr)
- 542 • Operating system(s): Platform independent
- 543 • Programming language: R (>= 4.2)
- 544 • Other requirements: katdetectr (1.1.2), MafTools (2.13.0), ClusteredMutations (1.0.1), kataegis
- 545 (0.99.2), SeqKat (0.0.8), SigProfilerClusters (1.0.11), dplyr (1.0.10), tidyr (1.2.1), ggplot2 (3.4.0),
- 546 variantAnnotation (1.44.0), mltools (0.3.5)
- 547 • License: GPL-3

## 548 **Author contributions**

549 Daan M. Hazelaar: Conceptualization, Data curation, Formal Analysis, Investigation, Methodology, Software,  
 550 Validation, Visualization, Writing – Original draft

551 Job van Riet: Conceptualization, Methodology, Investigation, Software, Visualization, Writing – review &  
552 editing

553 Youri Hoogstrate: Conceptualization, Methodology, Software, Writing - review & editing

554 Harmen J. G. van de Werken: Conceptualization, Funding acquisition, Investigation, Methodology, Project  
555 administration, Resources, Supervision, Writing - review & editing

## 556 Acknowledgments

557 We thank Martijn Lolkema, John Martens, Marcel Smid, Guido Jenster, and Stavros Makrodimitis for their  
558 discussions, input, and support. Additionally, we would like to thank Coen Berns and Yi Ping for their initial  
559 efforts in detecting kataegis.

## 560 References

- 561 [1] S. Nik-Zainal *et al.*, “Mutational Processes Molding the Genomes of 21 Breast Cancers,” *Cell*, vol. 149, no.  
562 5, pp. 979–993, May 2012, doi: 10.1016/j.cell.2012.04.024.
- 563 [2] L. B. Alexandrov *et al.*, “Signatures of mutational processes in human cancer,” *Nature*, vol. 500, no. 7463,  
564 Art. no. 7463, Aug. 2013, doi: 10.1038/nature12477.
- 565 [3] P. J. Campbell *et al.*, “Pan-cancer analysis of whole genomes,” *Nature*, vol. 578, no. 7793, Art. no. 7793,  
566 Feb. 2020, doi: 10.1038/s41586-020-1969-6.
- 567 [4] L. B. Alexandrov *et al.*, “The repertoire of mutational signatures in human cancer,” *Nature*, vol. 578, no.  
568 7793, Art. no. 7793, Feb. 2020, doi: 10.1038/s41586-020-1943-3.
- 569 [5] E. N. Bergstrom *et al.*, “Mapping clustered mutations in cancer reveals APOBEC3 mutagenesis of  
570 ecDNA,” *Nature*, vol. 602, no. 7897, Art. no. 7897, Feb. 2022, doi: 10.1038/s41586-022-04398-6.
- 571 [6] M. B. Burns *et al.*, “APOBEC3B is an enzymatic source of mutation in breast cancer,” *Nature*, vol. 494, no.  
572 7437, Art. no. 7437, Feb. 2013, doi: 10.1038/nature11881.
- 573 [7] D. Mas-Ponte and F. Supek, “DNA mismatch repair promotes APOBEC3-mediated diffuse hypermutation  
574 in human cancers,” *Nat Genet*, vol. 52, no. 9, Art. no. 9, Sep. 2020, doi: 10.1038/s41588-020-0674-6.
- 575 [8] S.-Y. Lee, H. Wang, H. J. Cho, R. Xi, and T.-M. Kim, “The shaping of cancer genomes with the regional  
576 impact of mutation processes,” *Exp Mol Med*, vol. 54, no. 7, Art. no. 7, Jul. 2022, doi: 10.1038/s12276-  
577 022-00808-x.
- 578 [9] S. A. Roberts *et al.*, “Clustered Mutations in Yeast and in Human Cancers Can Arise from Damaged Long  
579 Single-Strand DNA Regions,” *Molecular Cell*, vol. 46, no. 4, pp. 424–435, May 2012, doi:  
580 10.1016/j.molcel.2012.03.030.
- 581 [10] A. Mayakonda, D.-C. Lin, Y. Assenov, C. Plass, and H. P. Koeffler, “Maftools: efficient and comprehensive  
582 analysis of somatic variants in cancer,” *Genome Res.*, vol. 28, no. 11, pp. 1747–1756, Nov. 2018, doi:  
583 10.1101/gr.239244.118.
- 584 [11] D. Lora, “ClusteredMutations: Location and Visualization of Clustered Somatic Mutations.” Apr. 29, 2016.  
585 Accessed: Nov. 28, 2022. [Online]. Available: <https://CRAN.R-project.org/package=ClusteredMutations>
- 586 [12] X. Lin *et al.*, “kataegis: an R package for identification and visualization of the genomic localized  
587 hypermutation regions using high-throughput sequencing,” *BMC Genomics*, vol. 22, no. 1, p. 440, Jun.  
588 2021, doi: 10.1186/s12864-021-07696-x.
- 589 [13] F. Yousif, X. Lin, F. Fan, C. Lalansingh, and J. Macdonald, “SeqKat: Detection of Kataegis.” Mar. 11, 2020.  
590 Accessed: Nov. 28, 2022. [Online]. Available: <https://CRAN.R-project.org/package=SeqKat>
- 591 [14] E. N. Bergstrom, M. Kundu, N. Tbeileh, and L. B. Alexandrov, “Examining clustered somatic mutations  
592 with SigProfilerClusters,” *Bioinformatics*, vol. 38, no. 13, pp. 3470–3473, Jul. 2022, doi:  
593 10.1093/bioinformatics/btac335.

- 594 [15] R. Killick, P. Fearnhead, and I. A. Eckley, "Optimal Detection of Changepoints With a Linear  
595 Computational Cost," *Journal of the American Statistical Association*, vol. 107, no. 500, pp. 1590–1598,  
596 Dec. 2012, doi: 10.1080/01621459.2012.737745.
- 597 [16] A. J. Scott and M. Knott, "A Cluster Analysis Method for Grouping Means in the Analysis of Variance,"  
598 *Biometrics*, vol. 30, no. 3, pp. 507–512, 1974, doi: 10.2307/2529204.
- 599 [17] I. E. Auger and C. E. Lawrence, "Algorithms for the optimal identification of segment neighborhoods,"  
600 *Bulletin of Mathematical Biology*, vol. 51, no. 1, pp. 39–54, Jan. 1989, doi: 10.1016/S0092-  
601 8240(89)80047-3.
- 602 [18] P. Selenica *et al.*, "APOBEC mutagenesis, kataegis, chromothripsis in EGFR-mutant osimertinib-resistant  
603 lung adenocarcinomas," *Annals of Oncology*, vol. 33, no. 12, pp. 1284–1295, Dec. 2022, doi:  
604 10.1016/j.annonc.2022.09.151.
- 605 [19] A. Stenman, M. Yang, J. O. Paulsson, J. Zedenius, K. Paulsson, and C. C. Juhlin, "Pan-Genomic Sequencing  
606 Reveals Actionable CDKN2A/2B Deletions and Kataegis in Anaplastic Thyroid Carcinoma," *Cancers*, vol.  
607 13, no. 24, Art. no. 24, Jan. 2021, doi: 10.3390/cancers13246340.
- 608 [20] P. Priestley *et al.*, "Pan-cancer whole-genome analyses of metastatic solid tumours," *Nature*, vol. 575,  
609 no. 7781, Art. no. 7781, Nov. 2019, doi: 10.1038/s41586-019-1689-y.
- 610 [21] D. M. Hazelaar and J. van Riet, "Characterization and Visualization of Kataegis in Sequencing Data. R  
611 package version 1.2.0." [Online]. Available: <https://doi.org/doi:10.18129/B9.bioc.katdetectr>.
- 612 [22] J. Van Riet and D. Hazelaar, "ErasmusMC-CCBC/evaluation\_katdetectr: Publication." Zenodo, Sep. 08,  
613 2023. doi: 10.5281/ZENODO.8328463.
- 614 [23] R Core Team, *R: A Language and Environment for Statistical Computing*. Vienna, Austria: R Foundation  
615 for Statistical Computing, 2022. [Online]. Available: <https://www.R-project.org/>
- 616 [24] R. Killick and I. Eckley, "changepoint:an R package for changepoint analysis," *Journal of Statistical  
617 Software*, vol. 58, no. 3, Art. no. 3, 2014.
- 618 [25] R. Killick, K. Haynes, and I. A. Eckley, *changepoint: An R package for changepoint analysis software  
619 reference*. 2022. [Online]. Available: <https://CRAN.R-project.org/package=changepoint>
- 620 [26] D. Chicco and G. Jurman, "The advantages of the Matthews correlation coefficient (MCC) over F1 score  
621 and accuracy in binary classification evaluation," *BMC Genomics*, vol. 21, no. 1, p. 6, Jan. 2020, doi:  
622 10.1186/s12864-019-6413-7.
- 623 [27] D. Hazelaar, J. van Riet, and H. van de Werken, "Datasets used for the performance evaluation of  
624 kataegis detection tools." Zenodo, Jun. 08, 2022. doi: 10.5281/ZENODO.8046959.
- 625 [28] Hazelaar DM; van Riet J; Hoogstrate Y; van de Werken HJG. Supporting data for "Katdetectr: An  
626 R/Bioconductor package utilizing unsupervised changepoint analysis for robust kataegis detection";  
627 GigaScience Database 2023. <http://dx.doi.org/10.5524/102445>

628

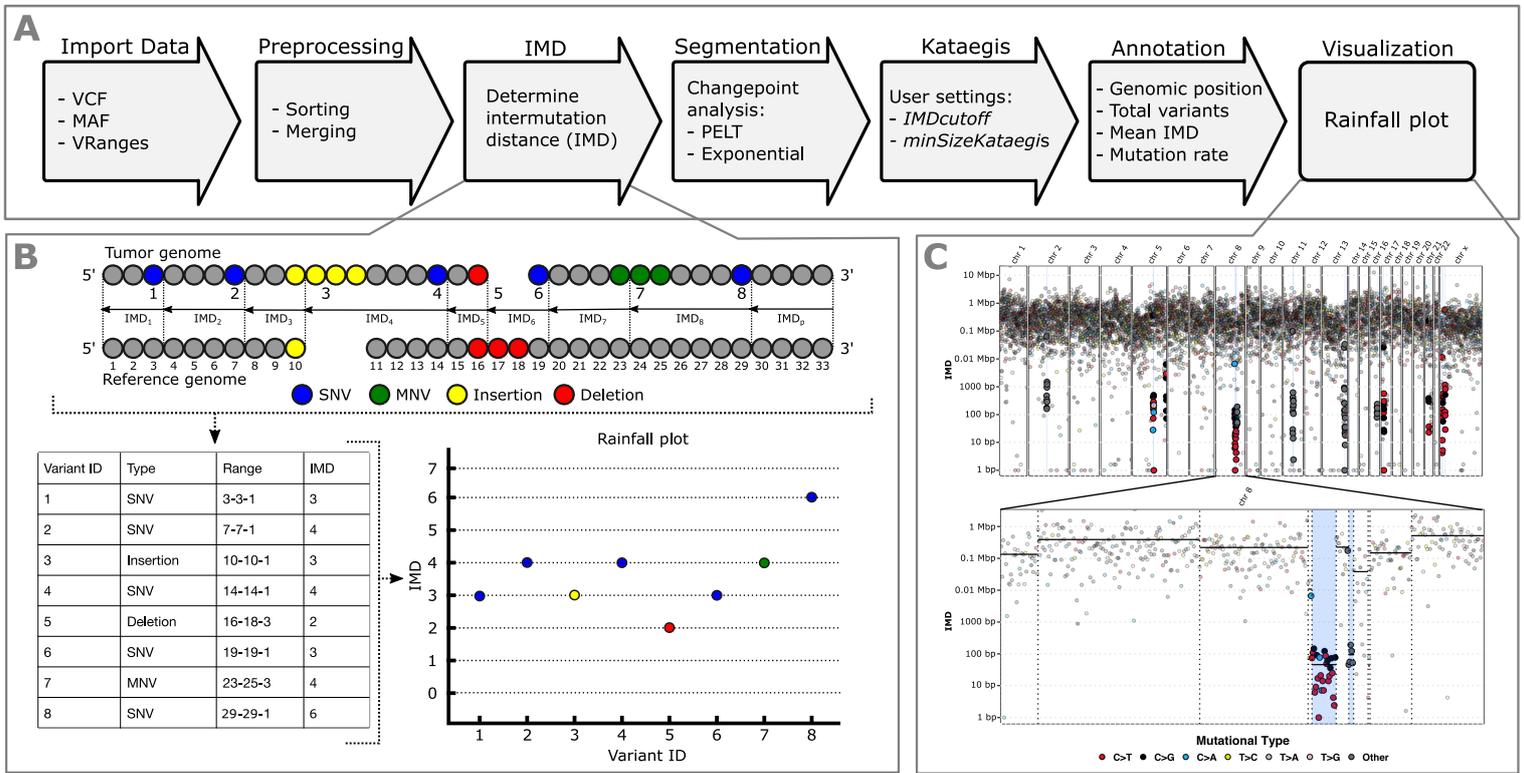


Figure 3

[Click here to access/download;Figure;figure\\_3\\_rainfall\\_plots.pdf](#)

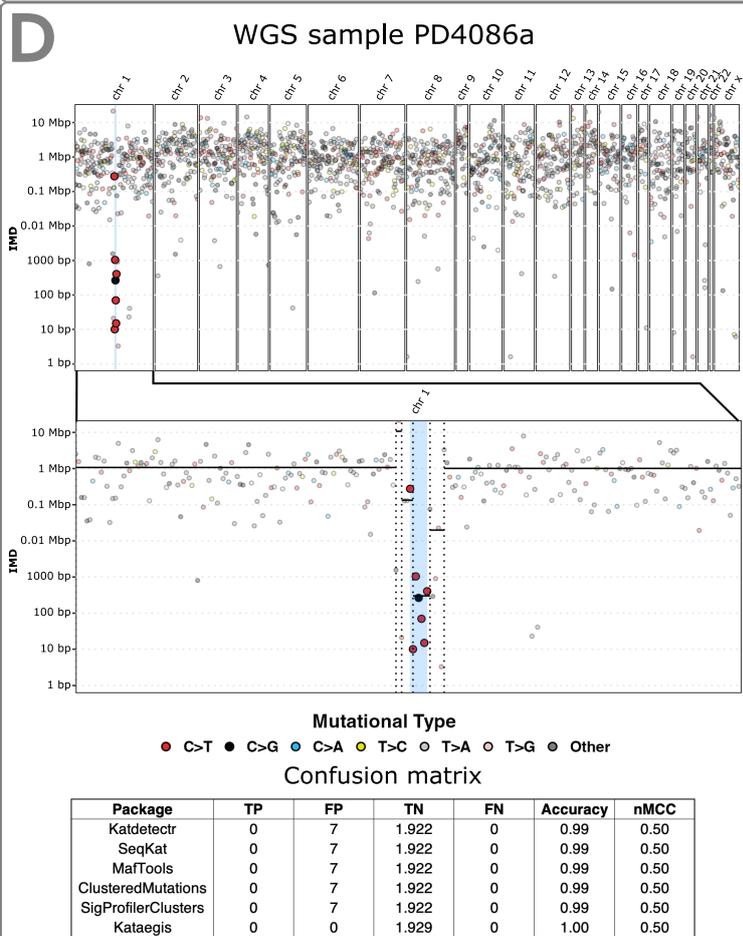
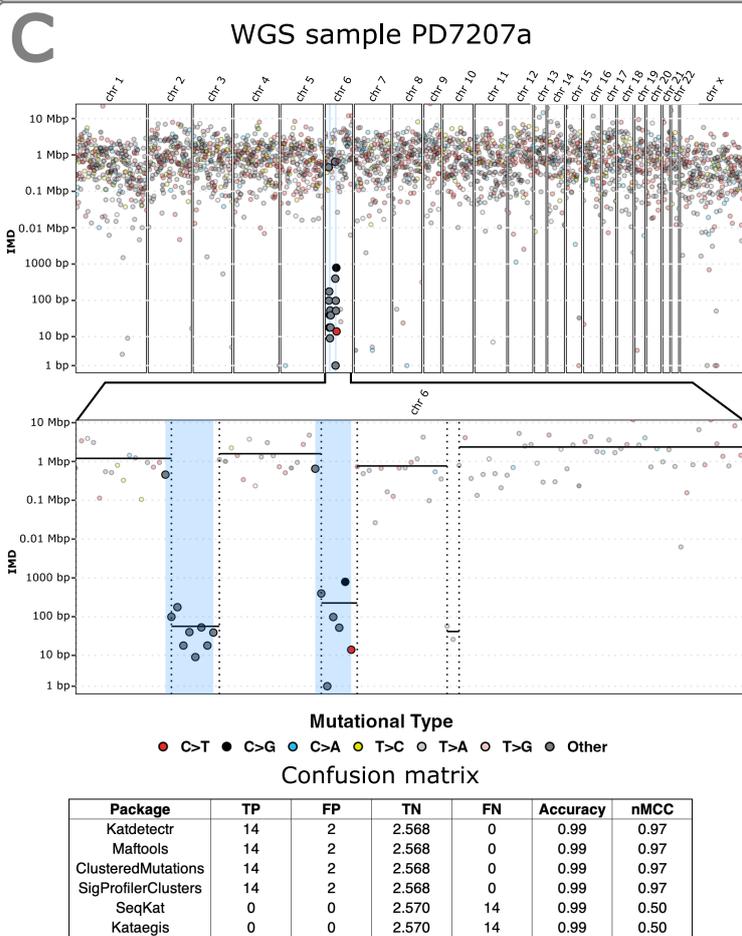
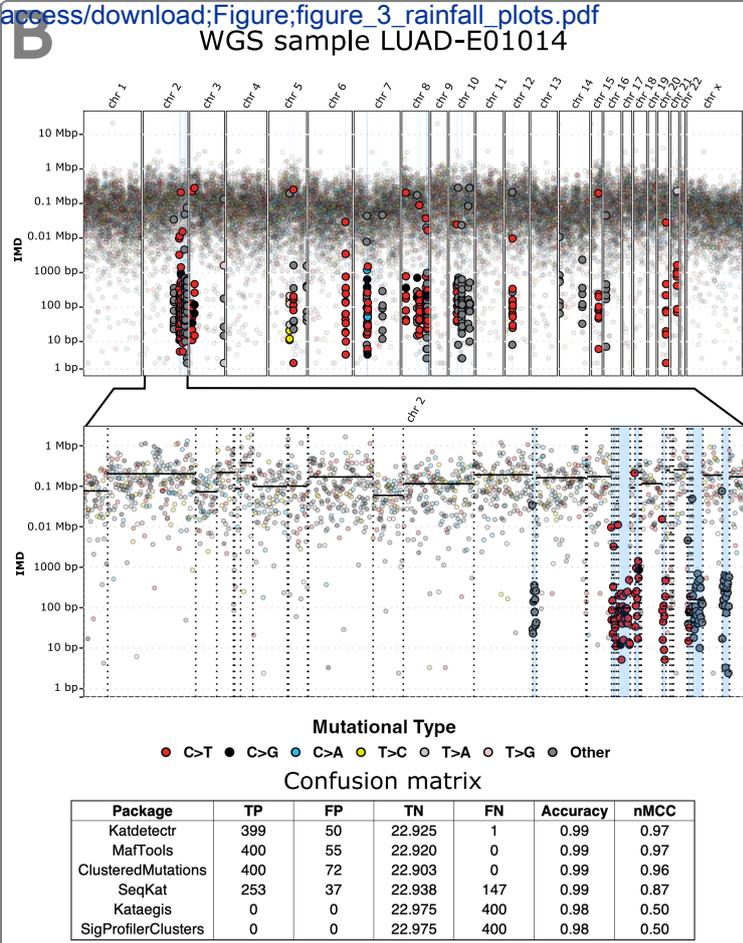
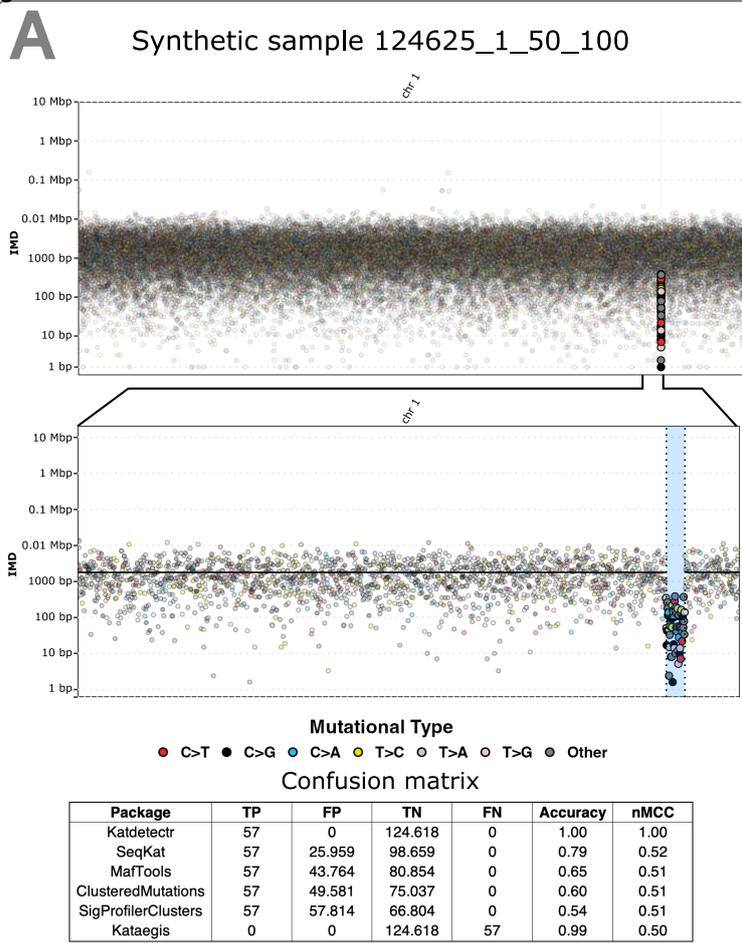
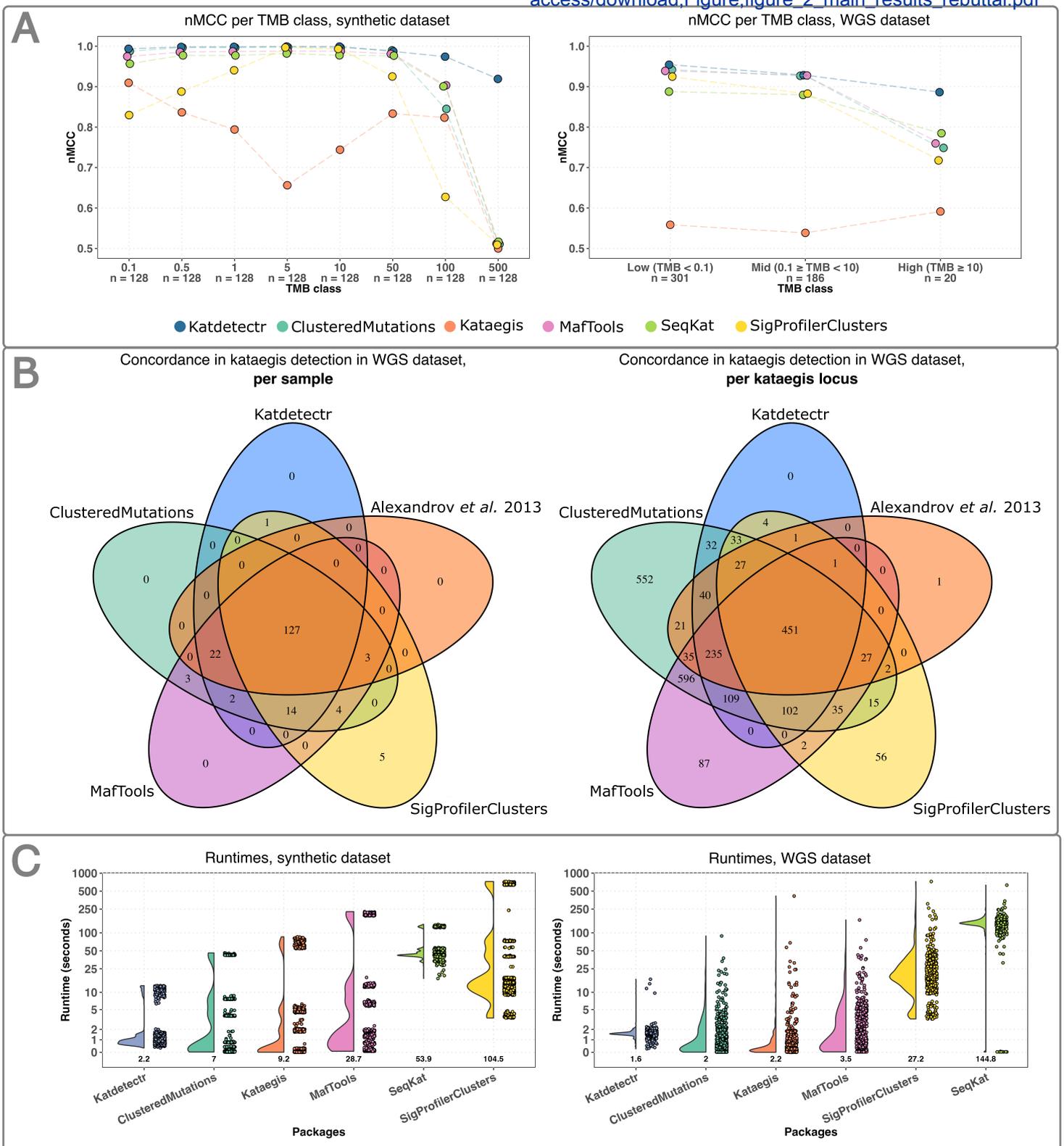


Figure 2

[Click here to access/download:Figure:figure\\_2\\_main\\_results\\_rebuttal.pdf](https://access/download/Figure:figure_2_main_results_rebuttal.pdf)

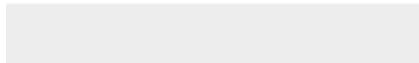




Click here to access/download

**Supplementary Material**

[supplementary\\_material\\_vignette\\_general\\_overview.pdf](#)





Click here to access/download  
**Supplementary Material**  
supplementary\_material\_figure\_1.docx



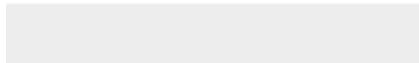


Click here to access/download  
**Supplementary Material**  
supplementary\_material\_figure\_2.docx



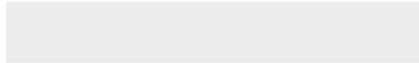


Click here to access/download  
**Supplementary Material**  
supplemental\_material\_figure\_3.docx





Click here to access/download  
**Supplementary Material**  
supplementary\_material\_table\_1.docx





Click here to access/download  
**Supplementary Material**  
supplementary\_material\_table\_2.docx





Click here to access/download  
**Supplementary Material**  
rebuttal\_katdetectr\_gigascience.pdf

